# –Supporting information–
# Compression-induced anti-nematic order in glassy and semicrystalline polymers

Sara Jabbari-Farouji and Damien Vandembroucq

## Generation and characterization of polymer configurations

The large-scale melt samples are obtained from replications of the equilibrated melt samples generated in a cubic box with an initial length $L_0$ with final dimensions $(L_x, L_y, L_z) = (n_x L_0, n_y L_0, n_z L_0)$. We have chosen $L_0$ to be at least four times the radius of gyration of polymers to avoid spatial separation of long chains due to wrapping of coordinates in a periodic box. The information regarding the box size of initial melt configurations and the the replicated samples are given in the Table S1. The large-scale melt samples are subsequently cooled down to $T = 0.2$ at cooling-rates $10^{-6}\,\tau^{-1}$ and $10^{-3}\,\tau^{-1}$ to obtain semicrystalline and glassy configurations, respectively. The gyration radii of polymers in the melts state $T = 1$ and in the semicrystalline and glassy states at $T = 0.2$ are also reported in the Table S1.

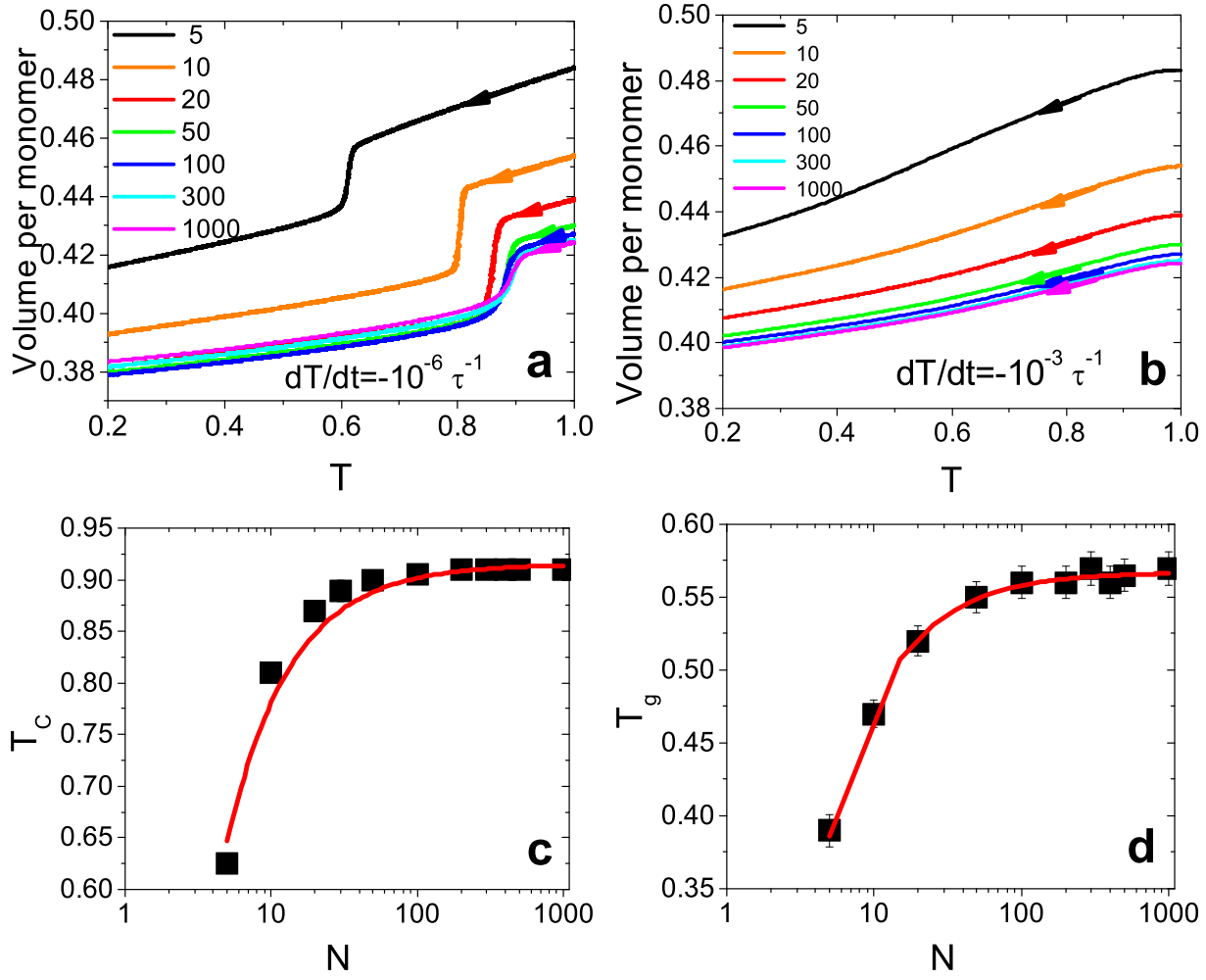


Figure S1: Volume per monomer $v$ as a function of $T$ for different chain lengths $5 \leq N \leq 1000$ obtained at constant cooling-rates a) $\dot{T} = -10^{-6}, \tau^{-1}$ and b) $\dot{T} = -10^{-3}\,\tau^{-1}$, respectively. Panels c) and d) show the crystallization temperature $T_c$ and the glass transition temperature $T_g$ versus $N$, respectively. The solid lines show fits to the Flory-Fox equation [2].

For the slower cooling rate, we observe crystallization characterized by a drastic drop of volume per monomer $v$ drops drastically. We define the crystallization temperature $T_c$ as the temperature that marks the onset of the abrupt drop of $v$ upon cooling, see Fig. S1 (a). For the rapid quench of $\dot{T} = -10^{-3}\ \tau^{-1}$, the volume changes with $T$ are less abrupt, see Fig. S1 (b). Polymers retain their amorphous configurations and undergo a glass transition. We define glass transition temperature $T_g$ as the inflection point of the $v - T$ curve for which its slope changes. Figures S1(c) and S1 (d) present the extracted values of $T_c$ and $T_g$ versus $N$. Both $T_c$ and $T_g$ increase with $N$, and

| $N$ | $n_{c0}$ | $R_g/\sigma$ melt | $L_0$ | $n_c$ replicated | $L_x$ replicated | $L_y$ replicated | $L_z$ replicated | $R_g/\sigma$ crys | $R_g/\sigma$ glass | $\Phi_c$ | $L_{\rm crys}/\sigma$ | $N_{\rm tie}$ |
|---|---|---|---|---|---|---|---|---|---|---|---|---|
| 5 | 2000 | 0.615 | 16.9 | 128000 | 67.6 | 67.6 | 67.6 | 0.70 | 0.68 | 0.5 | 18.8 | 0 |
| 20 | 1000 | 1.79 | 20.6 | 27000 | 61.8 | 61.8 | 61.8 | 2.78 | 1.94 | 0.75 | 47.9 | 5.4 |
| 50 | 1000 | 3.17 | 27.8 | 18000 | 83.4 | 83.4 | 55.6 | 4.56 | 3.26 | 0.6 | 37.3 | 10 |
| 300 | 300 | 8.25 | 33.7 | 3600 | 67.4 | 67.4 | 101.1 | 9.11 | 8.10 | 0.43 | 15.4 | 21 |
| 1000 | 500 | 15.11 | 59.6 | 2000 | 119.2 | 119.2 | 59.6 | 15.45 | 14.90 | 0.36 | 14.3 | 27 |

Table S1: Summary of polymer melt configurations used in the simulations. $N$ is the number of monomers in a chain, $n_{c0}$ the number of chains used for the melt equilibration and $n_c$ is the number of chains in the replicated melt samples that are further cooled to obtain glassy and semicrystalline polymers. $L_x$, $L_y$ and $L_z$ represent the dimensions of replicated box. We also report the value of average gyration radii $R_g = \sqrt{\langle R_g^2 \rangle}$ and the average linear dimension of crystalline domains $L_{\rm crys}$ and average size of tie chains $N_{\rm tie}$, *i.e.* the number of monomers in amorphous strands connecting two distinct crystalline domains.

their dependence is well described by the phenomenological Flory-Fox equation [2] of the form $T_{c,g} = T_{c,g}^{\infty} - K_{c,g}/N$. We find $T_c^{\infty} = 0.915 \pm 0.005$ and $K_c = 1.34 \pm 0.06$ for the semicrystalline polymers and $T_g^{\infty} = 0.567 \pm 0.005$ and $K_g = 0.90 \pm 0.02$ for the glassy polymers. The observed $N$-dependence of $T_c$ and $T_g$ is well-known and is related to the effects of chain ends on interfacial energies and free volume [2].

To characterize the crystallites, we use the notion of *crystalline domains* which are defined as a set of spatially connected regions with the same orientation [3]. To identify the crystalline domains, we divide the box into cells of size about $2\sigma$ and we compute the nematic tensor $Q_{\alpha\beta} = 1/N \sum_i (3/2 b_\alpha^i b_\beta^i - 1/2 \delta_{\alpha\beta})$ of unit bond vectors of polymers $b^i$ within each cell. The largest eigenvalue and the corresponding eigenvector of the nematic tensor determine the local order parameter $S_{\rm loc}$ and the preferred orientation of bonds, *i.e.* director $\widehat{\mathbf{u}}$ in each cell. The volume fraction of cells with $S_{\rm loc} > 0.8$ defines the degree of *crystallinity* $\Phi_C$ also included in Table S1. We perform a cluster analysis [4] by merging two neighbouring cells if they are both crystalline and their directors share the same orientation within the threshold $\widehat{\mathbf{u}}_i \cdot \widehat{\mathbf{u}}_j \geq 0.97$. From the volume distribution of crystallites, we determine the average volume of crystalline domains $\langle V_{\rm domain} \rangle$ and hence their average linear dimension as $L_{\rm crys} = \langle V_{\rm domain} \rangle^{1/3}$. Characterization of the crystalline domains allows us to directly identify tie chains as the chain segments connecting them [5]. The average length of tie-chains $N_{\rm tie}$ are also given in Table S1.

**Volume changes during the tensile and compressive deformation**

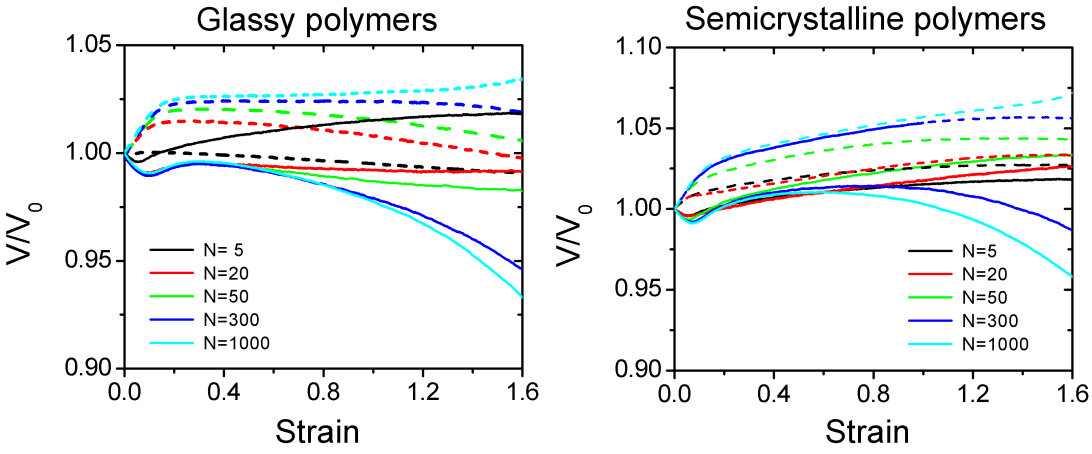


Figure S2: The ratio of sample volumes $V$ relative to their undeformed volume $V_0$ against strain magnitude from uniaxial compression (solid lines) and tensile (dashed lines) deformation for (a) glassy and (b) semicrystalline polymers with chain lengths $N = 5$, 20, 50, 300 and 1000 as given in the legends.

**Stress-strain curves shifted by flow stress**

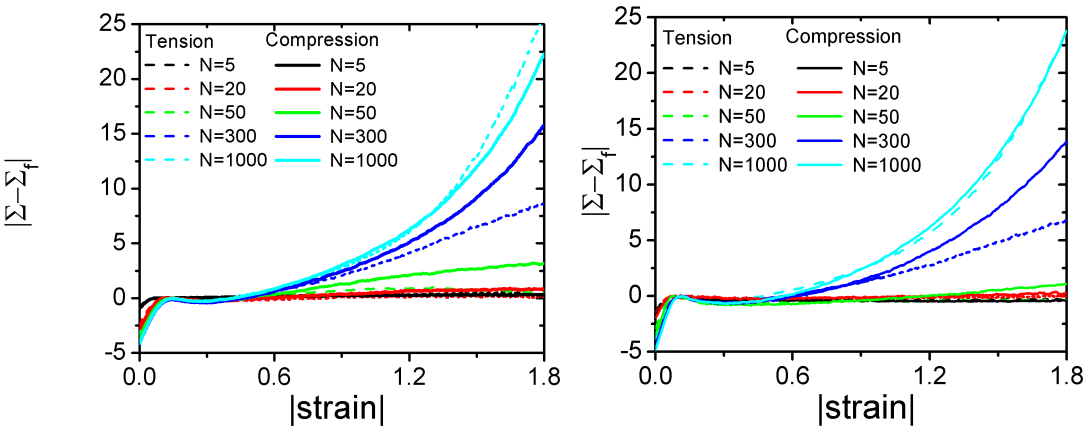


Figure S3. The stress response of (a) glassy and (b) semicrystalline polymers shifted by their corresponding flow stress values $\Sigma_f$ under uniaxial compression (solid lines) and tensile (dashed lines) deformation for different chain lengths $N = 5$, 20, 50, 300 and 1000 as given in the legends.

### Conformational changes of semicrystalline polymers of chain length $N = 50$ under deformation

Considering that the entanglement length of polymers of CG-PVA model is $N_e \approx 40$ and the average stem length of long semicrystalline polymers is about 30, the polymeric samples of $N = 50$ lie in the crossover region from unentangled to entangled regimes and also from a fully extended to a chain-folded regime with several folds. The intrachain bond-bond orientational correlation functions of fully extended short chains $N < 30$ are always positive whereas those of longer chains with several folds exhibit a minimum around the average length of folds (stem length), see Fig. 3 in the main article. The undeformed semicrystalline polymers of $N = 50$ are at the intermediate regime, where the chains make only one fold at most, see Fig. S4. Hence, their intrachain bond-bond orientational correlation functions become negative for a range of curvilinear distances $n \geq 20$. This feature persists even for the deformed semicrystalline samples as presented in Fig. S5.

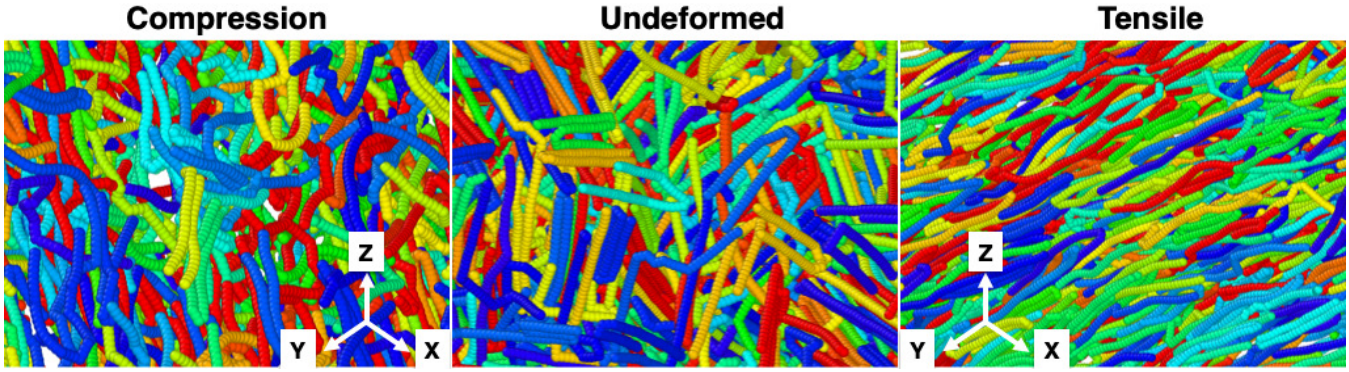


Figure S4. Snapshots of conformations of semicrystalline polymers $N = 50$ under compression $\epsilon = -1.6$, undeformed $\epsilon = 0$ and under tension $\epsilon = 1.6$.

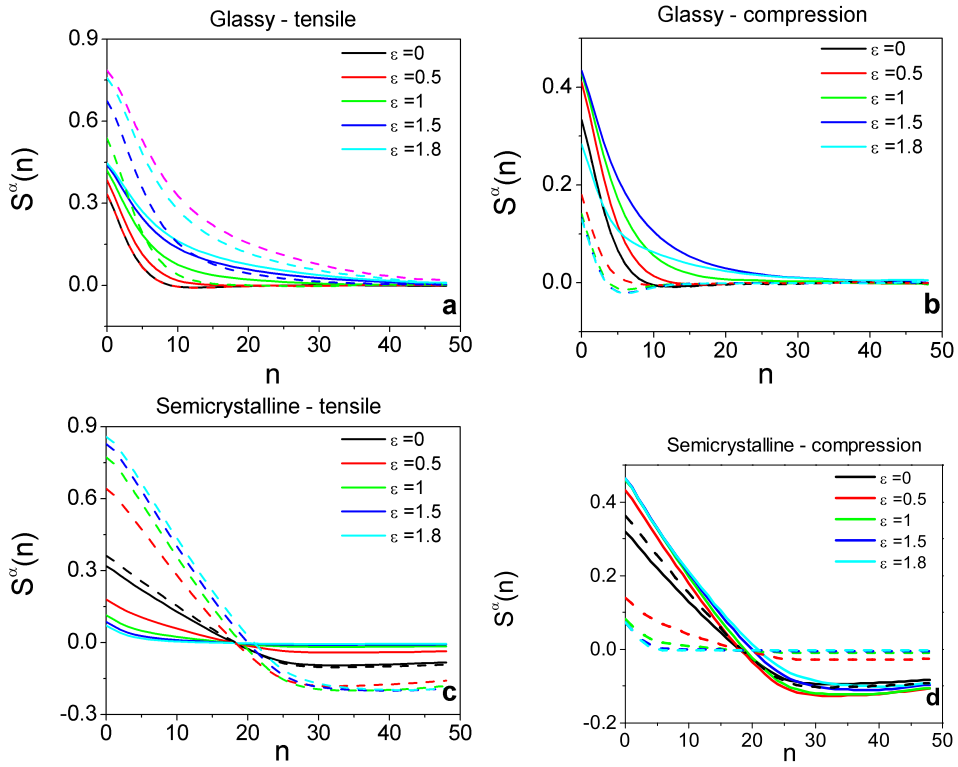


Figure S5. Evolution of anisotropic intrachain bond-bond orientational correlation functions against the curvilinear distance $n$ along chain backbones at different tensile and compressive strain magnitudes $\varepsilon$ for glassy (a and b) and semicrystalline polymers (c and d) with chain length $N = 50$. The dashed lines depict the intrachain correlations parallel to the deformation axis $S^{||}(n) \equiv S^{y}(n)$ and the solid lines correspond to the average intrachain correlations in the perpendicular directions $S^{\perp}(n) \equiv \big(S^{x}(n) + S^{z}(n)\big)/2$.

**Changes of crystallinity degree with strain**

We present the evolution of crystallinity degree $\Phi_c$ as a function of strain value for both compressive (negative strains) and tensile (positive strains) deformation modes. First, we note that $\Phi_c$ of undeformed samples is a non-monotonic function of chain lengths. It increase with $N$ for short unentangled chains due to the reduction of interfacial free energy whereas it decreases with $N$ upon entanglement of chains for $N > N_e$ where $N_e \approx 40$. Nonetheless, we observe a general trend for changes of $\Phi_c$ with strain. Under tension, $\Phi_c$ initially exhibits a small decrease due to reorientation and fragmentation of crystallites [6] and then increases as a result of chain alignment with the deformation axis. On the contrary, compression-induced anti-nematic ordering of the bonds, leads to reduction of $\Phi_c$. This is particularly remarkable for long chains $N = 300$ and 1000 where the $\Phi_c$ approaches zero at large compressive strains demonstrating a complete destruction of crystalline order.

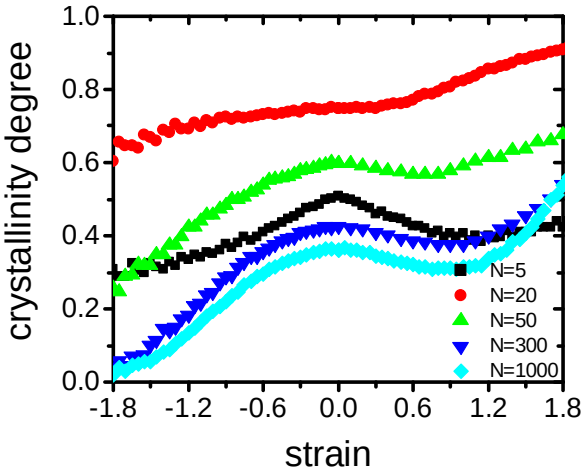


Figure S6. The evolution of crystallinity degree $\Phi_c$ as a function of strain for different chain lengths $N$ as shown in the legend.

[1] Meyer, H.; Müller-Plathe, F. J. Chem. Phys. 2001, 115, 7807.
[2] T. G. Fox and P. J. Flory, Journal of Applied Physics 1950, 21, 581.
[3] Luo, C.; Sommer, J.-U. J. Polym. Sci., Part B: Polym. Phys. 2010,48, 2222–2232.
[4] S. Jabbari-Farouji, J. Rottler, O. Lame, A. Makke, M. Perez and J. L. Barrat, Journal of Physics: Condensed Matter, 2015, 27, 194131.
[5] S. Jabbari-Farouji, O. Lame, M. Perez, J. Rottler and J.-L. Barrat, Phys. Rev. Lett., 2017, 118, 217802.
[6] S. Jabbari-Farouji, J. Rottler, O. Lame, A. Makke, M. Perez and J. L. Barrat, ACS Macro Letters, 2015, 4, 147–151.